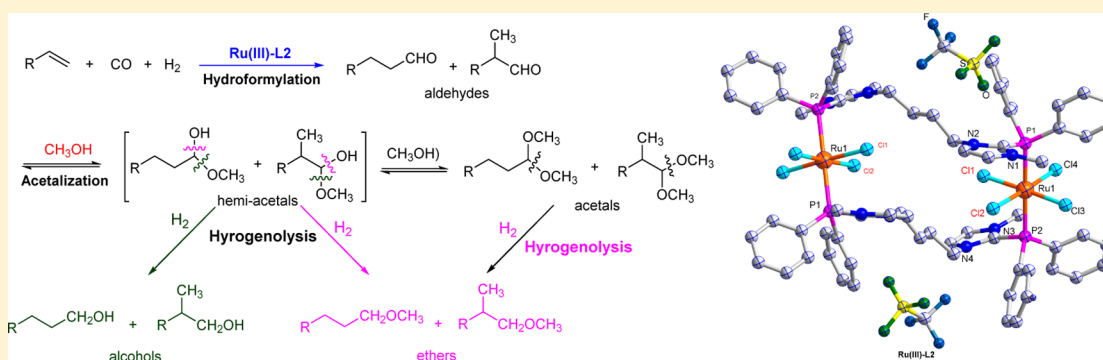# Production of Alcohols from Olefins via One-Pot Tandem Hydroformylation−Acetalization−Hydrogenolysis over Bifunctional Catalyst Merging Ru^{III}−P Complex and Ru^{III} Lewis Acid

Peng Wang, Dong-Liang Wang, Huan Liu, Xiao-Li Zhao, Yong Lu, and Ye Liu*

Shanghai Key Laboratory of Green Chemistry and Chemical Processes, School of Chemistry and Molecular Engineering, East China Normal University, 3663 North Zhongshan Road, Shanghai 200062, PR China

Ⓢ *Supporting Information*

ABSTRACT: A novel three-step tandem hydroformylation−acetalization−hydrogenolysis was first proposed to produce alcohols (derivatives) from olefins, and the developed unique Ru(III)-complex [Ru(III)-L2] ligated by the ionic diphosphine (L2) proved efficient toward this tandem reaction. In Ru(III)-L2, the strong π-acceptor nature of L2 guaranteed Ru-center remaining in +3 valence state without redox reaction. Hence, Ru(III)-L2 was able to behave as a bifunctional catalyst merging Ru^{III}−P complex and Ru^{III} Lewis acid, which acted not only as a transition metal catalyst responsible for hydroformylation of olefins and hydrogenolysis of (hemi)acetals but also as a Ru³⁺ Lewis acid in charge of acetalization of aldehydes [to form (hemi)acetals]. The easily performed acetalization served as a bridge step to get through the pathway from aldehydes to alcohols instead of the direct hydrogenation.

INTRODUCTION

Current industrial production of alcohols mainly employs a two-step process including hydroformylation of olefin in syngas to aldehydes and then hydrogenation of aldehydes to alcohols in H_2.[1,2] One-pot tandem hydroformylation−hydrogenation reaction is a practical alternative to achieve valuable and stable alcohols under hydroformylation conditions with advantages of simplified process operation and using syngas as the source of hydrogenation instead of pure hydrogen.[3−8] In the reported two-step tandem hydroformylation−hydrogenation, transition metals such as Ru,[9−11] Rh−Ru,[3−6] and Rh[7,8,12−15] with the aid of auxiliary phosphine ligands are commonly used catalytic systems. In these examples, cocatalysis[16,17] using Rh−Ru bimetallic systems by Bell et al.[3] and Nozaki et al.,[4−6] supermolecular ligand-based Rh-catalysts by Breit et al.[7,8] or two cooperative ligand-based Rh-catalysts by Cole-Hamilton et al.[12] is the basic concept to enable the hydroformylation-related tandem reactions under the compatible reaction conditions. Compared to high-cost rhodium as the preferred catalysts for hydroformylation[1] but low activity toward hydrogenation in the presence of CO gas,[3−6] the inexpensive ruthenium-catalysts not only exhibit high activities toward hydrogenation of alde-

hydes[18,19] even in the presence of syngas[20] but also are employed as alternatives for hydroformylation.[9−11]

Besides hydrogenation of aldehydes to afford alcohols, hydrogenolysis of ketals/acetals is another pathway to obtain alcohols (or the corresponding ethers) over acidic transition metal catalysts.[21−24] Inspired by the facts including hydrogenolysis of acetals to yield alcohols (or ethers) and the successful hyroformylation−acetalization over the bifunctional catalyst reported by us,[25,26] we first proposed a three-step tandem reaction to produce alcohols (derivatives) from olefins via hydroformylation of olefins, acetalization of aldehydes, and hydrogenolysis of acetals (Scheme 1). In this tandem process, the easily accomplished acetalization served as a transition step to get through the pathway from aldehydes to alcohols instead of direct hydrogenation. Since cocatalysis of compatible bifunctional catalysts is basically required to fulfill the tandem reaction, herein through simple complexation of a unique ionic diphosphine (L2) with cheap hydrated RuCl₃·3H₂O, a novel Ru(III)-complex, [Ru(III)-L2], was developed for the

Scheme 1. Tandem Hydroformylation–Acetalization–Hydrogenolysis for Production of Alcohols (and Its Ethers) from Olefins over Ru(III)-L2 as the Efficient Bifunctional Catalyst
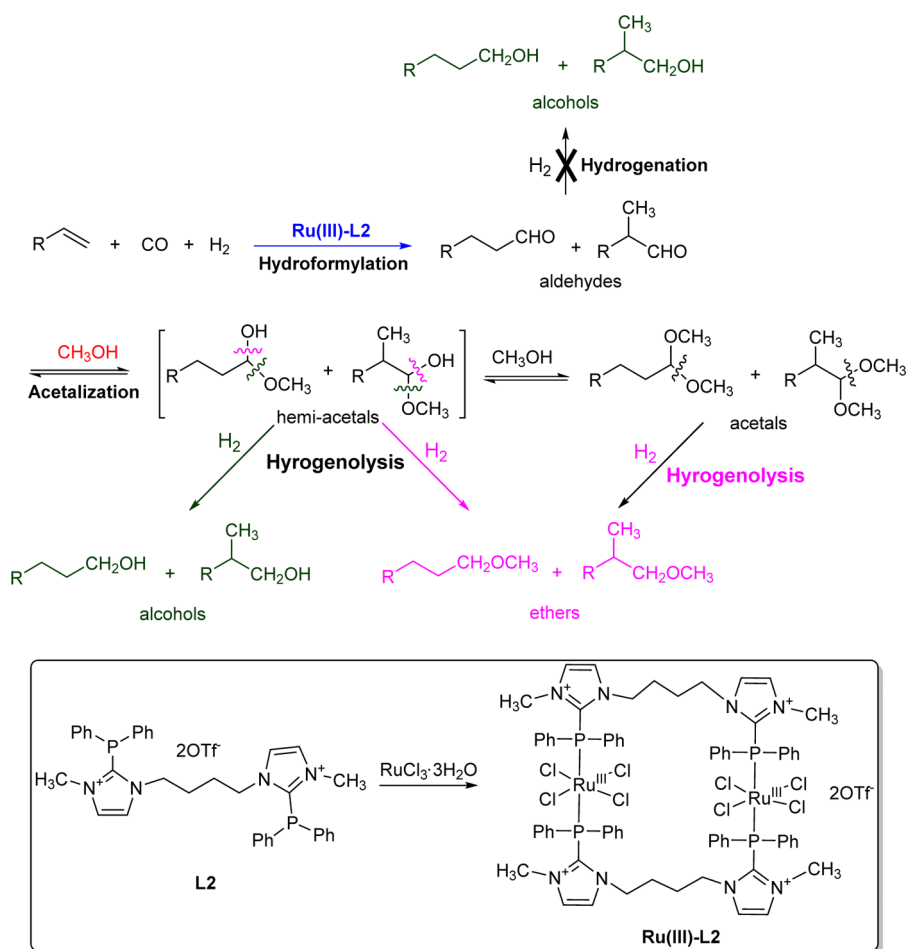

proposed three-step tandem reaction. As for [**Ru(III)-L2**], the strong π-acceptor nature of **L2** guaranteed Ru-center remaining in +3 valence state without redox reaction. Hence, **Ru(III)-L2** was able to behave as a bifunctional catalyst merging Ru^III–P complex and Ru^III Lewis acid, which acted not only as a transition metal catalyst responsible for hydroformylation of olefins and hydrogenolysis of (hemi)acetals but also as a Ru³⁺ Lewis acid in charge of acetalization of aldehydes [to form (hemi)acetals] (Scheme 1). Compared to Rh-catalysts, the low-cost Ru³⁺-catalyst with stronger Lewis acidity will more favor acetalization and hydrogenolysis.

RESULTS AND DISCUSSION

Synthesis and Characterization of Ru^III-Complexes of Ru(III)-L1 and Ru(III)-L2. It has been known that the complexation of RuCl₃·3H₂O with typical electron-rich phosphines with strong σ-donor ability never result in paramagnetic Ru(III)-complexes[27,28] due to the potential redox reaction. Herein, the complexation of RuCl₃·3H₂O with the ionic phosphines of **L1** (monophosphine) and **L2** (diphosphine) in MeOH only led to the formation of **Ru(III)-L1** and **Ru(III)-L2** with unchanged +3 valence state for Ru-center. These ionic Ru^III-complexes were air- and moisture-stable in the solid state for several weeks under ambient condition. As for **L1** and **L2**, due to the strong electron-withdrawing effect of the neighbored positive-charged imidazoliums, they are very intensive π-acceptor ligands (See

Figure S1 as analytic evidence). The molecular structures of **Ru(III)-L1**[29] and **Ru(III)-L2** analyzed by the single crystal X-ray diffraction were depicted in Figure 1. In these two Ru^III-complexes, the Ru(III) (d⁵) ion is situated exactly in the center of octahedron, which is six-coordinated by four Cl⁻ in the equatorial plane and two imidazolium-tailed phosphino-fragments in the axial positions. In **Ru(III)-L2**, the two Ru-ions were linked by two **L2** to form a distorted quadrilateral configuration. Diphosphine **L2** is not chelated to the same Ru-center but serves as a bridge to the two Ru-ions. From another perspective, **Ru(III)-L2** was like an analogue of two **Ru(III)-L1** molecules standing shoulder to shoulder. However, the Ru–P and Ru–Cl bond distances observed in **Ru(III)-L1** and **Ru(III)-L2** are completely different. As for **Ru(III)-L2**, when two Ru³⁺ ions are linked by two **L2** to form a distorted quadrilateral ring structure, the Ru–Cl and Ru–P bond distances are universally longer than those in **Ru(III)-L1**, which is supposed to be unstable. Especially of note is that the two Ru–Cl bond oriented inside the quadrilateral ring are dramatically weakened with indication of the much longer Ru–Cl bond distances (Ru–Cl1, 2.3755(12) Å; Ru–Cl2, 2.3806(13) Å). The fused ring-configuration of the two highly symmetrical octahedral Ru-complex units facilitates its stability. In addition, **Ru(IIII)-L2** is featured with paramagnetic nature due to the presence of one unpaired electron in the Ru(III) center. Its ¹H NMR and ³¹P NMR signals attributed to **L2** are broadened to flatness.
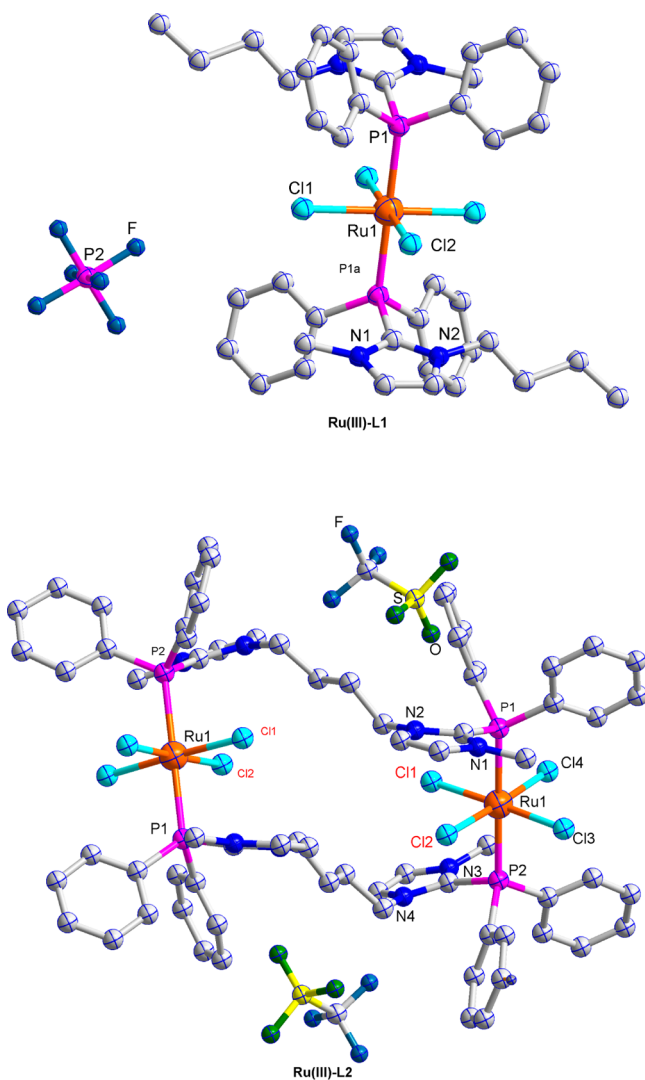
Figure 1. Molecular structures of **Ru(III)-L1** and **Ru(III)-L2**. H atoms and the solvent molecules were omitted for clarity. [Selected bond distances, Å: **Ru(III)-L1**, Ru1−P1 2.4055(9); Ru1−Cl12.3442(9); Ru1−Cl22.3615(9). **Ru(III)-L2**, Ru1−P1 2.4107(14); Ru1−P2 2.4121(14); Ru1−Cl1 2.3755(12); Ru1−Cl2 2.3806(13); Ru1−Cl3 2.3599(12); Ru1−Cl4 2.3573(12)].

The complexation of commercial RuCl$_3$·3H$_2$O with the neutral diphosphine of **L2′** could not afford the expected stable complex analogue of **Ru(III)-L2′**. It was found that in the course of separation and purification of **Ru(III)-L2′** in open air the Ru-blacks were gradually precipitated from the solution indicating the serious decomposition of this complex. This result further demonstrated that in **Ru(III)-L2** complex the ionic diphosphine of **L2** could render the corresponding Ru-complex good stability due to its increased π-acceptor ability to develop π-backdonation in Ru−P linkages.

Tandem Hydroformylation−Acetalization−Hydrogenolysis of Olefins over Bifunctional Ru^{III}-Catalytic System. The tandem hydroformylation−acetalization−hydrogenolysis of 1-octene in MeOH as the model reaction was first investigated over the as-synthesized complexes of **Ru(III)-L1** and **Ru(III)-L2** (Table 1). Compared to **Ru(III)-L1** with nonanol selectivity of 28%, the much higher nonanol selectivity of 72% was observed over **Ru(III)-L2** accompanied by the much lower selectivities to a mixture of internal octenes and
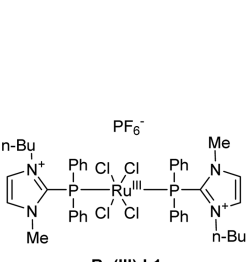
nonanals (sel.$_{internal-octenes}$ = 11%, sel.$_{nonanals}$ = 2%), indicating that the reaction rate for hydroformylation of internal octenes and acetalization of nonanals were greatly accelerated by **Ru(III)-L2**. Under the same conditions, the **Ru(III)-L2** *in situ* formed by mixing RuCl$_3$·3H$_2$O and **L2** at molar ratio of 1/2 exhibited the same activity as the as-synthesized one (entry 3). Then, the mixture of RuCl$_3$·3H$_2$O and **L2** was applied in place of as-synthesized **Ru(III)-L2** to evaluate the effects of different reaction factors. Under the optimal conditions (P/Ru = 2/5 molar ratio, syngas 4.0 MPa, 120 °C), the total selectivities to nonanols and nonyl-methyl ethers over **L2**-RuCl$_3$·3H$_2$O system reached 96% along with 99% conversion of 1-octenes when the reaction time was prolonged to 48 h (entry 7).

The profiles of 1-octene conversion and nonanols (derivatives) selectivity versus reaction time in Figure 2 further indicated that in first 4 h 98% 1-octene was isomerized to a mixture of internal octenes over **L2**-based RuCl$_3$·3H$_2$O catalyst (99% conversion of 1-octene and 99% selectivity to internal octenes). Later on, the resultant internal octenes gradually converted to nonanals via Ru(III)-P complex catalyzed hydroformylation and then to the acetals via subsequent acetalization with MeOH catalyzed by Lewis acidic Ru^{3+}-center. The formed acetals with reversible transformation to the hemiacetals were hydrogenolyzed smoothly to yield nonanols or nonanyl-methyl ethers via C−OCH$_3$ or C−OH bond cleavage over the same RuCl$_3$·3H$_2$O/**L2** catalytic system (Scheme 1).
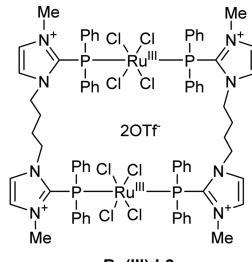
Reasonably, the replacement of MeOH by DMF just stopped the reaction at the hydroformylation step due to impossibility for formation of (hemi)acetal intermediates responsible for subsequent transformation to nananols or the corresponding ethers via hydrogenolysis (entry 8). Without the presence of **L2** in RuCl$_3$·3H$_2$O, only the isomerization of 1-octene to a mixture of internal octenes dominantly happened (entry 8, conv. = 97%, sel.$_{internal-octenes}$ = 71%) (entry 9 vs 5), indicating the indispensable role of the phosphine ligand in transition metal catalysis for hydroformylation.

While the tandem hydroformylation−acetalization−hydrogenolysis was repeated under the same reaction conditions by using the other phosphines such as **L1**, **L2′**, dppb, or PPh$_3$, the sluggish conversions of a mixture of internal octenes to nonanals dramatically limited the subsequent acetalization and hydrogenolysis, leading to the very low selectivities to nonanols and the ethers (entries 10−13 vs 1). It was noted that although **L1** and **L2** had the very similar σ-donor ability (see Figure S1) they exhibited quite different activities toward the tandem reaction. The molecular structural information in Figure 1 indicated that the two of Ru−Cl bond distances of [Ru−Cl1, 2.3755(12) Å; Ru−Cl1, 2.3803(13) Å] oriented inside the distorted quadrilateral ring in **Ru(III)-L2** were uniquely lengthened in comparison to those in **Ru(III)-L1** [Ru−Cl, 2.3442(9), 2.3615(9) Å]. As a result, the four weakened Ru−Cl bonds in **Ru(III)-L2** were able easily ruptured to provide unsaturation site for coordination of CO and the olefin to facilitate the formation of Ru−acyl complex intermediates responsible for the efficient hydroformylation. Meanwhile, the exposed Ru^{3+} after easy cleavage of Cl$^−$ could exhibit its Lewis acidity effectively. In addition, the spacy six-coordinate octahedral configuration for **Ru(III)-L2** also favored the coordination of the branched internal octenes to Ru(III) center rather than the typical Ru(0,II)-complexes such as Ru$_3$(CO)$_{12}$ or Ru(COD)Cl$_2$ typically with five-coordinated structures. Hence, when Ru$_3$(CO)$_{12}$ and Ru(COD)Cl$_2$ were
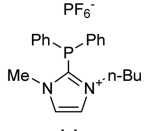
Table 1. Tandem Hydroformylation−Acetalization−Hydrogenolysis of 1-Octene Catalyzed by RuCl$_3$·3H$_2$O under Different Conditions[a]
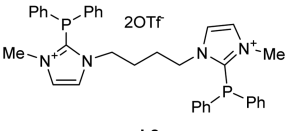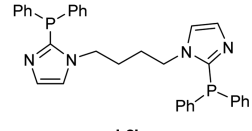
| entry | catalytic system | sol. | time (h) | P/Ru | conv. (%)[b] | sel.oxo (%)[b,c] | | | | sel. internal-octenes (%)[b,c] | sel.octanes (%)[b,c] | L/B oxo[d] |
						sel.nonanals	sel.acetals	sel.alcohol	sel.ether			
1	**Ru(III)-L1**	MeOH	48	2/1	96	17	9	28	14	29	3	0.5
2	**Ru(III)-L2**	MeOH	48	2/1	97	2	2	72	11	11	2	0.7
3	RuCl$_3$·3H$_2$O + **L2**	MeOH	48	2/1	97	1	2	73	10	1	2	0.7
4	RuCl$_3$·3H$_2$O + **L2**	MeOH	24	2/1	99	2	22	58	11	6	1	0.5
5	RuCl$_3$·3H$_2$O + **L2**	MeOH	24	2/5	99		20	67	9	3	1	0.7
6	RuCl$_3$·3H$_2$O + **L2**	MeOH	24	1/5	96	4	17	54	21	2	2	0.7
7	RuCl$_3$·3H$_2$O + **L2**	MeOH	48	2/5	99		2	88	8	1	1	0.6
8	RuCl$_3$·3H$_2$O + **L2**	DMF	24	2/5	99	89				9	2	0.5
9	RuCl$_3$·3H$_2$O	MeOH	24		97	16	2	8	2	71	1	0.6
10	RuCl$_3$·3H$_2$O + **L1**	MeOH	24	2/5	93	7	24	32	10	24	3	0.7
11	RuCl$_3$·3H$_2$O + **L2′**	MeOH	24	2/5	98	12	4	34	6	42	2	0.5
12	RuCl$_3$·3H$_2$O + dppb	MeOH	24	2/5	96	13	17	20	10	38	2	0.6
13	RuCl$_3$·3H$_2$O + PPh$_3$	MeOH	24	2/5	99	3	15	26	12	43	1	0.7
14[e]	Ru$_3$(CO)$_{12}$ + **L2**	MeOH	24	2/5	98	14	7			76	3	0.5
15[f]	Ru(COD)Cl$_2$ + **L2**	MeOH	24	2/5	99	8	6			78	7	0.7
16[g]	Rh(acac) (CO)$_2$ + **L2**	MeOH	48	2/5	98	16	28			46	10	0.7
17[h]	RuCl$_3$·3H$_2$O + **L2**	MeOH + 1-nonanol	48	2/5								

[a]**Ru(III)−L1** 0.15 mmol, **Ru(III)−L2** 0.075 mmol, RuCl$_3$·3H$_2$O 0.15 mmol, **L2** or dppb 0.03 mmol, **L1** 0.06 mmol (P/Ru = 2/5 molar ratio), 1-octene 5 mmol, CO/H$_2$ (1:1) 4.0 MPa, 120 °C, solvent 3 mL. [b]Determined by GC with *n*-dodecane as internal standard. [c]S_{oxo} (%) = selectivities to oxo-products including nonanals, acetals, nonanols, and methyl-nonyl ethers, which were determined by normalization method. [d]L/B$_{oxo}$ = selectivities to linear oxo-products/selectivities to branched oxo-products. [e]Ru$_3$(CO)$_{12}$ 0.05 mmol, **L2** 0.03 mmol. [f]Ru(COD)Cl$_2$ 0.15 mmol, **L2** 0.03 mmol. [g]Rh(acac) (CO)$_2$ 0.15 mmol, **L2** 0.03 mmol. [h]The reaction of 1-nonanol (5 mmol) and methanol (3 mL) without the presence of 1-octene was performed under the same conditions as in entry 7.
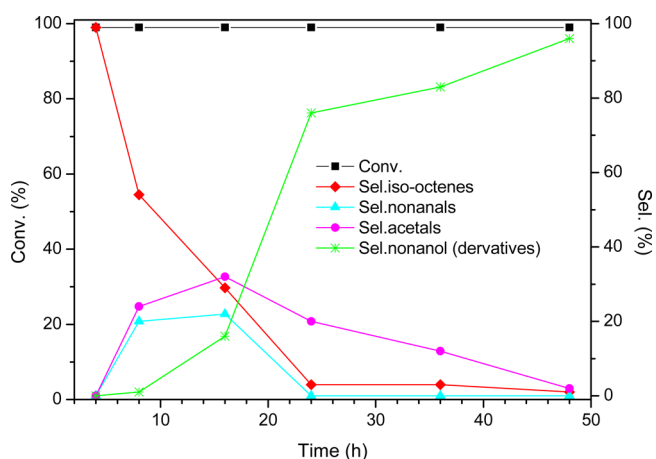
Figure 2. Evolution profiles of 1-octene conversion and product selectivity distribution vs reaction time catalyzed by **L2**-based RuCl$_3$·3H$_2$O system.

applied to replace Lewis acidic RuCl$_3$·3H$_2$O even with the presence of **L2**, the hydroformylation of internal octenes was inefficient (entries 14 and 15: sel. internal-octene = 76−78%). The

use of Rh(acac)(CO)$_2$ with the presence of **L2** gave rise to the formation of neither nonanals nor nonanols (entry 14). It means that the hydrogenolysis of (hemi)acetals was completely inhibited over the low valence state Ru(0, I)/Rh(I)-catalysts. In addition, the reaction of 1-nonanol and methanol without the presence of 1-octene was also carried out under the same conditions (entry 17). The obtained result indicated that etherification between 1-nonanol and methanol did not happened at all over RuCl$_3$·3H$_2$O/**L2** system, which further confirmed that the observed methyl-nonyl ethers in entry 7 indeed came from hydrogenolysis of (hemi)acetals.

In order to clarify the role of **L2**-based Ru^{III}-catalyst for each reaction step via tandem hydroformylation−acetalization−hydrogenolysis, the acetalization−hydrogenolysis of 1-nonanal (commercial) with MeOH and hydrogenolysis of 1,1-dimethoxynonane (commercial), respectively, were conducted over **L2**-based RuCl$_3$·3H$_2$O (Tables 2 and 3). It was indicated that the reaction of 1-nonanal with MeOH indeed yielded 1-nonanol as the major product whether in syngas or pure H$_2$ via tandem acetalization−hydrogenolysis over acidic **L2**-based RuCl$_3$·3H$_2$O system (Table 2, entries 1 and 2). Over the same catalytic system, the absence of MeOH led to no conversion of 1-nonanal (entries 5 and 6), ruling out the

Table 2. Acetalization−Hydrogenolysis of 1-Nonanal (Commercial) under Different Conditions[a]
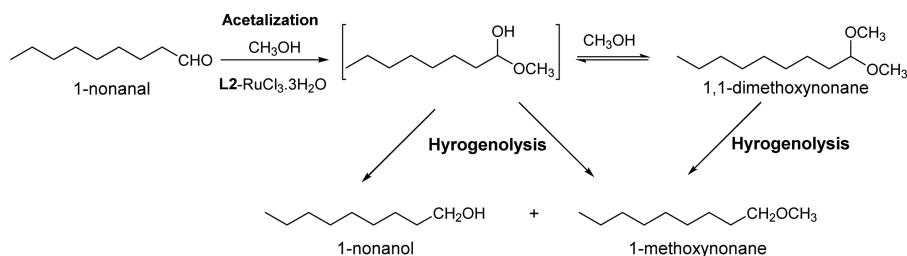
entry	RuCl$_3$·3H$_2$O	L2	CO/H$_2$[b]	H$_2$[b]	conv.[c]	sel.$_{acetal}$ (%)[c]	sel.$_{alcohol}$ (%)[c]	sel.$_{ether}$ (%)[c]
1	√	√	√	−	100	13	64	23
2	√	√	−	√	100	11	83	6
3	√	−	−	√	100	91	8	1
4	−	√	−	√	−	−	−	−
5[d]	√	√	√	−	−	−	−	−
6[d]	√	√	−	√	−	−	−	−

[a]RuCl$_3$·3H$_2$O 0.15 mmol (3 mol %), L2 0.03 mmol (P/Ru = 2/5 molar ratio), 1-nonanal (or 1,1-dimethoxyoctane) 5 mmol, 120 °C, CH$_3$OH 3 mL, 48 h; [b]CO/H$_2$ 4.0 MPa or H$_2$ 4.0 MPa; [c]Determined by GC analysis calibrated with the authentic sample; [d]The reaction was conducted without presence of MeOH.

Table 3. Hydrogenolysis of 1,1-Dimethoxynonane under Different Conditions[a]
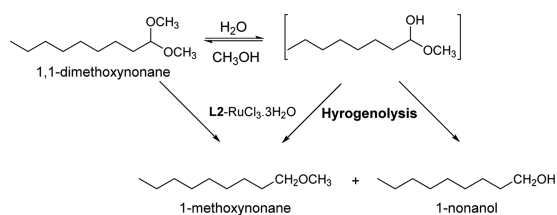
entry	RuCl$_3$·3H$_2$O	L2	CO/H$_2$[b]	H$_2$[b]	conv.[c]	sel.$_{alcohol}$ (%)[c]	sel.$_{ether}$ (%)[c]
1	√	√	√	−	90	26	74
2	√	√	−	√	94	90	10
3	√	−	−	√	11	100	−
4	−	√	−	√	36	92	8

[a]RuCl$_3$·3H$_2$O 0.15 mmol (3 mol %), L2 0.03 mmol (P/Ru = 2/5 molar ratio), 1-nonanal (or 1,1-dimethoxyoctane) 5 mmol, 120 °C, CH$_3$OH 3 mL, 48 h. [b]CO/H$_2$ 4.0 MPa, H$_2$ 4.0 MPa. [c]Determined by GC analysis calibrated with the authentic samples.

possibility for direct hydrogenation in syngas or pure H$_2$, and 1,1-dimethoxynonane was directly hydrogenolized in MeOH to 1-nonanol and 1-methoxynonane with the aid of L2-based RuCl$_3$·3H$_2$O system (Table 3, entries 1 and 2). Comparatively,

in pure H$_2$ (4.0 MPa), most of 1,1-dimethoxynonane was hydrogenolyed to 1-nonanol with 90 selectivity (entry 2 vs 1). The presence of Lewis acidic RuCl$_3$·3H$_2$O was a must for acetalization and hydrogenolysis (entry 4 in Tables 2 and 3), and the presence of L2 could greatly improve the reaction rate for hydrogenolysis of 1,1-dimethoxynonane (entry 3 in Tables 2 and 3. Undoubtedly, over L2-based RuCl$_3$·3H$_2$O system, acetalization of aldehydes and the consequent hydrogenolysis were carried out definitely against direct hydrogenation of aldehydes.

The generality of L2-RuCl$_3$·3H$_2$O system for the three-step tandem reaction was explored on the scope of different alcohols and olefins (Table 4). Over L2-RuCl$_3$·3H$_2$O, the preceding hydroformylation of olefins all preformed smoothly without sensitive discrimination on the steric and electronic effects of the applied olefins. However, when EtOH and i-PrOH were applied instead of MeOH, the increased steric hindrance slowed down the reaction rate for the subsequent acetalization and hydrogenolysis, leading to the decreased selectivities to nonanol accompanied by the increased selectivities to acetals (entry 2) or nonanals (entry 3). It was noted that the use of i-PrOH only corresponded to the formation of nonanols (sel. 69%) without the presence of nonanyl-(iso-)propyl ethers, indicating the absolute cleavage of C−O(iPr) bond in the hemiacetals due to the bulky steric hindrance. When glycol was

Table 4. Generality of RuCl$_3$·3H$_2$O/L2 Catalytic System for Tandem Hydroformylation−Acetalization−Hydrogenolysis of Olefins in Alcohols[a]

entry	olefin	alcohol (sol.)	conv. (%)[b]	sel.$_{oxo}$ (%)[b,c]				sel.$_{internal-octene}$ (%)[b,c]	sel.$_{alkane}$ (%)[b,c]	L/B$_{oxo}$[d]
				sel.$_{aldehydes}$	sel.$_{acetals}$	sel.$_{alcohols}$	sel.$_{ethers}$			
1	1-octene	MeOH	99		2	88	8	1	1	0.6
2	1-octene	EtOH	99	6	14	66	9	4	1	0.6
3	1-octene	i-PrOH	98	27		69		3	1	0.6
4	1-octene	glycol	99		90			9	1	0.5
5	cyclooctene	MeOH	99			93	4		3	
6	styrene	MeOH	99		18	60	14		8	1.1
7	2,5-dihydrofuran	MeOH	92		14	71	7		8	

[a]RuCl$_3$·3H$_2$O 0.15 mmol, L2 0.03 mmol (P/Ru = 2/5 molar ratio), olefin 5 mmol, alcohol 3 mL, CO/H$_2$ (1:1) 4.0 MPa, temp 120 °C, reaction time 48 h; [b]Determined by GC and GC-Mass; [c]S$_{oxo}$ (%) = selectivities to oxo-products including aldehydes, acetals, alcohols, and ethers; [d]L/B$_{oxo}$ = selectivities to linear oxo-products/selectivities to branched oxo-products.

Table 5. Crystal Data and Structure Refinement for Ru(III)-L1 and Ru(III)-L2

	Ru(III)-L1[29]	Ru(III)-L2
empirical formula	$C_{46}H_{60}Cl_4N_4O_2P_2Ru \cdot PF_6$	$C_{72}H_{76}Cl_8N_8P_4Ru_2 \cdot 2CF_3SO_3$
formula weight	1150.76	1961.17
crystal system	monoclinic	monoclinic
space group	$C2/c$	$C2/c$
a (Å)	25.2640(9)	35.044(3)
b (Å)	9.7111(3)	8.9810(7)
c (Å)	22.9382(8)	33.426(3)
α (deg)	90	90
β (deg)	104.148	111.446
γ (deg)	90	90
V (Å^3)	5457.0(3)	9791.8(14)
Z	4	4
d_{calc} (g cm^{-3})	1.401	1.330
μ (Mo Kα) (mm^{-1})	0.630	0.693
T (K)	296(2)	173(2)
λ	0.71073	0.71073
total reflections	30584	42073
unique reflections (R_{int})	4777 (0.0219)	8584 (0.1121)
R_1 [$I > 2\sigma(I)$]	0.0449	0.0527
wR_2 (all data)	0.1354	0.1201
$F(000)$	2364	3976

applied to repeat this tandem reaction, due to the presence of thermodynamically stable five-member 1,3 dioxolanyl ring in the formed acetal products, the subsequent hydrogenolysis of such stable acetals was completely inhibited, resulting in 90% selectivity to the acetals without any formation of nonanols and the ethers (entry 4). As for the olefins without isomerization phenomenon, the tandem reactions all proceeded smoothly along with good selectivities to alcohols and the corresponding ethers (entries 5−7).

■ **CONCLUSION**

Over the developed novel ionic diphosphine (**L2**)-based RuCl$_3$· 3H$_2$O system, the three-step tandem hydroformylation−acetalization−hydrogenolysis was first proven to be an absolutely preferred pathway to tandem hydroformylation−hydrogenation for the production of alcohols from olefins. **L2**-based RuCl$_3$·3H$_2$O system served as an efficient bifunctional catalyst merging Lewis acid (Ru^{3+}) and Ru^{III}−P complex. In **L2**-based RuCl$_3$·3H$_2$O system, the typical π-acceptor nature of **L2** with very weak reductive ability kept Ru-center always in +3 valence state without redox reaction. In this way, the (*in situ*) formed **Ru(III)-L2** complex with a unique distorted quadrilateral ring structure was in charge of efficient hydroformylation of olefins and hydrogenolysis of (hemi)acetals. In addition, the Lewis acidity of the fully exposed Ru^{3+} ion also played indispensible role in promoting acetalization of aldehydes and the subsequent hydrogenolysis of (hemi)acetals to yield the alcohols and the corresponding ethers.

■ **EXPERIMENTAL SECTION**

Reagents and Analysis. The chemical reagents were purchased from Shanghai Aladdin Chemical Reagent Co., Ltd., and Alfa Aesar China and used as received. FT-IR spectra were recorded on a Nicolet NEXUS 670 spectrometer. The ^{1}H and ^{31}P NMR spectra for the analyses of the common compounds were recorded on a Bruker Avance 500 spectrometer. The ^{31}P NMR spectra for the analyses of the phosphine-selenides (as shown in Figure S1) were recorded on a Bruker Avance 500 spectrometer. The ^{31}P NMR spectra were referenced to 85% H$_3$PO$_4$ sealed in a capillary tube as an internal

standard. Gas chromatography (GC) was performed on a SHIMADZU-2014 equipped with a DM-Wax capillary column (30 m × 0.25 mm × 0.25 μm). GC-mass spectrometry (GC-MS) was recorded on an Agilent 6890 instrument equipped with an Agilent 5973 mass selective detector. CHN-elemental analyses were obtained using an Elementar Vario EL III instrument.

Synthesis. **L1** and **Ru(III)-L1** were synthesized according to the method reported by us before.[29]

L2 and **Ru(III)-L2** were synthesized according to the following procedures: Under N$_2$ atmosphere, 1H-imidazole (13.6 g, 200 mmol) and 1,4-dibromobutane (22 g, 102 mmol) were added sequentially into the distilled water (100 mL), and then NaOH(8.0 g, 200 mmol) and (n-Bu)$_4$N$^+$Br$^-$ (33.4 mg, 0.1 mmol) were added into the mixtures. Next, the mixture was stirred vigorously at room temperature for 48 h. After cooling down to room temperature, the reaction mixture was treated with 400 mL of deionized water and then extracted with ethyl acetate (200 mL × 4). The combined organic phase was dried with anhydrous sodium sulfate. The residue after removal of the organic solvent in vacuo was then purified through silica gel column chromatography to give 1-(4-(1H-imidazol-1-yl)butyl)-1H-imidazole as the white powder (19.0 g, yield 98 wt %).

Then, under nitrogen atmosphere, a solution of 1-(4-(1H-imidazol-1-yl)butyl)-1H-imidazole (1.9 g, 10 mmol) in 50 mL of absolute THF (refluxed with sodium and distilled freshly before use) was cooled to −78 °C, and 10 mL of n-BuLi (2.2 M in hexane, 22 mmol) was added dropwise. The obtained reaction mixture after stirring vigorously for 1 h was added with chlorodiphenylphosphine (PPh$_2$Cl, 4.4 g, 20 mmol) dropwise. The resultant suspension was stirred for another 1 h at −78 °C and then warmed up to room temperature naturally. After quenching excess n-BuLi with 100 mL of deionized water, the mixture was stripped of solvent in vacuo and then extracted with dichloromethane (100 mL × 3). The combined organic phase was dried by anhydrous sodium sulfate and concentrated under vacuum. The residue was purified by column chromatography to give a white solid as the product of **L2′** [(2-(diphenylphosphino)-1-(4-(2-(diphenylphosphino)-1H-imidazol-1-yl)butyl)-1H-imidazole)] with the yield of 80% (4.4 g). A solution of **L2′** (5.6 g, 10 mmol) in 50 mL of CH$_2$Cl$_2$ was cooled to −55 °C, and then MeOTf (3.2 g, 20 mmol) was added dropwise. The resultant suspension was stirred for another 1 h at −55 °C and then warmed up to room temperature naturally. Then, the mixture was stripped of solvent in vacuo and washed by diethyl ether to give a white solid as product **L2** in 85% yield (5.0 g). ^{1}H NMR (δ,

ppm, CDCl$_3$): 8.00 (s, 2 H, N$^+$CHCHN), 7.55 (s, 2H, N$^+$CHCHN), 7.47 (s, 12 H, H_{Ar}), 7.34−7.33 (m, 8 H, H_{Ar}), 4.23 (m, 4 H, NCH_2CH$_2$CH$_2$CH_2N), 3.48 (s, 6 H, N$^+$CH_3), 1.52 (s, 4 H, NCH$_2$CH_2CH_2CH$_2$N). ^{31}P (δ, ppm, CD$_3$COCD$_3$): −27.1 (s, PPh$_2$).

Ru(III)-L2 was obtained as a yellow solid (yield: 80%) by complexation of commercial RuCl$_3$·3H$_2$O with **L2** at room temperature according to the procedures as described in our previous work.[29] The sample suitable for X-ray diffraction analysis was obtained by recrystallization from acetone/n-hexane. FT-IR (KBr): 3167 (m), 3045 (m), 2935 (m), 2871 (m), 1641 (m), 1569 (m), 1486 (s), 1440 (s), 1267 (s), 1227 (s), 1150 (s), 1029 (s), 745 (s), 698 (s). CHN-elemental analysis (found, %): C, 45.32; H, 3.91; N, 5.71 (calcd: C, 45.47; H, 4.07; N, 5.63). The complexation of commercial RuCl$_3$·3H$_2$O with **L2′** could not isolate the stable complex, because Ru-blacks were formed during the procedure of filtering and washing by PE and diethyl ether during product purification. The complex **Ru-L2′** is more sensitive to air and moisture than **Ru-L2**.

X-ray Crystallography. Intensity data were collected at 296 K for **Ru(III)-L2** on a Bruker SMARTAPEX II diffractometer using graphite monochromated Mo Kα radiation (λ = 0.71073 Å). Data reduction included absorption corrections by the multiscan method. The structures were solved by direct methods and refined by full matrix least-squares using SHELXS-97,[30] with all non-hydrogen atoms refined anisotropically. Hydrogen atoms were added at their geometrically ideal positions and refined isotropically. The crystal data and refinement details of **Ru(III)-L1** and **Ru(III)-L2** were given in Table 5.

General Procedures for Hydroformylation−Acetalization−Hydrogenolysis of Olefin in Alcohol. In a typical experiment for tandem hydroformylation−acetalization−hydrogenolysis, the commercial RuCl$_3$·3H$_2$O (0.15 mmol) and the isolated **L2** (0.03 mmol) were added into methanol (3 mL, or the other alcohol) and 1-octene (5 mmol, or the other olefin) sequentially. The obtained mixture in a 50 mL Teflon-lined stainless steel autoclave was sealed and pressured by syngas to 4.0 MPa. The reaction mixture was stirred vigorously at the appointed temperature for some time. Upon completion, the autoclave was cooled down to room temperature and depressurized carefully. The reaction solution was analyzed by GC to determine the conversions (n-dodecane as internal standard), and the product selectivities (normalization method) calibrated by the authentic samples, and the products were further identified by GC-Mass.

ASSOCIATED CONTENT

Ⓢ Supporting Information

The Supporting Information associated with this article can be found online. The Supporting Information is available free of charge on the ACS Publications website at DOI: 10.1021/acs.organomet.7b00266.

(PDF)

Accession Codes

CCDC 1541651 contains the supplementary crystallographic data for this paper. These data can be obtained free of charge via www.ccdc.cam.ac.uk/data_request/cif, or by emailing data_request@ccdc.cam.ac.uk, or by contacting The Cambridge Crystallographic Data Centre, 12 Union Road, Cambridge CB2 1EZ, UK; fax: +44 1223 336033.

AUTHOR INFORMATION

Corresponding Author

*E-mail: yliu@chem.ecnu.edu.cn.

ORCID ⓘ

Peng Wang: 0000-0003-1217-4801

Dong-Liang Wang: 0000-0002-0424-9132

Huan Liu: 0000-0003-0801-3861

Xiao-Li Zhao: 0000-0002-4458-6432

Yong Lu: 0000-0002-5126-1476

Ye Liu: 0000-0003-3875-2913

Notes

The authors declare no competing financial interest.

ACKNOWLEDGMENTS

REFERENCES

(1) Franke, R.; Selent, D.; Börner, A. *Chem. Rev.* **2012**, *112*, 5675−5732.

(2) Eilbracht, P.; Bärfacker, L.; Buss, C.; Hollmann, C.; Kitsos-Rzychon, B. E.; Kranemann, C. L.; Rische, T.; Roggenbuck, R.; Schmidt, A. *Chem. Rev.* **1999**, *99*, 3329−3366.

(3) Zakzeski, J.; Lee, H. R.; Leung, Y. L.; Bell, A. T. *Appl. Catal., A* **2010**, *374*, 201−212.

(4) Takahashi, K.; Yamashita, M.; Nozaki, K. *J. Am. Chem. Soc.* **2012**, *134*, 18746−18757.

(5) Yuki, Y.; Takahashi, K.; Tanaka, Y.; Nozaki, K. *J. Am. Chem. Soc.* **2013**, *135*, 17393−17400.

(6) Takahashi, K.; Yamashita, M.; Ichihara, T.; Nakano, K.; Nozaki, K. *Angew. Chem., Int. Ed.* **2010**, *49*, 4488−4490.

(7) Diab, L.; Šmejkal, T.; Geier, J.; Breit, B. *Angew. Chem., Int. Ed.* **2009**, *48*, 8022−8026.

(8) Fuchs, D.; Rousseau, G.; Diab, L.; Gellrich, U.; Breit, B. *Angew. Chem., Int. Ed.* **2012**, *51*, 2178−2182.

(9) Fleischer, I.; Dyballa, K. M.; Jennerjahn, R.; Jackstell, R.; Franke, R.; Spannenberg, A.; Beller, M. *Angew. Chem., Int. Ed.* **2013**, *52*, 2949−2953.

(10) Wu, L.; Fleischer, I.; Jackstell, R.; Profir, I.; Franke, R.; Beller, M. *J. Am. Chem. Soc.* **2013**, *135*, 14306−14312.

(11) Rodrigues, C.; Delolo, F. G.; Norinder, J.; Börner, A.; Bogado, A. L.; Batista, A. A. *J. Mol. Catal. A: Chem.* **2017**, *426*, 586−592.

(12) Boogaerts, I. I. F.; White, D. F. S.; Cole-Hamilton, D. J. *Chem. Commun.* **2010**, *46*, 2194−2196.

(13) Sandee, A. J.; Reek, J. N. H.; Kamer, P. C. J.; van Leeuwen, P. W. N. M. *J. Am. Chem. Soc.* **2001**, *123*, 8468−8476.

(14) Ichihara, T.; Nakano, K.; Katayama, M.; Nozaki, K. *Chem. - Asian J.* **2008**, *3*, 1722−1728.

(15) Diebolt, O.; Müller, C.; Vogt, D. *Catal. Sci. Technol.* **2012**, *2*, 773−777.

(16) Allen, A. E.; MacMillan, D. W. C. *Chem. Sci.* **2012**, *3*, 633−658.

(17) Du, Z.; Shao, Z. *Chem. Soc. Rev.* **2013**, *42*, 1337−1378.

(18) Tan, X.; Wang, G.; Zhu, Z.; Ren, C.; Zhou, J.; Lv, H.; Zhang, X.; Chung, L. W.; Zhang, L.; Zhang, X. *Org. Lett.* **2016**, *18*, 1518−1521.

(19) Dupau, P.; Bonomo, L.; Kermorvan, L. *Angew. Chem., Int. Ed.* **2013**, *52*, 11347−11350.

(20) Takahashi, K.; Nozaki, K. *Org. Lett.* **2014**, *16*, 5846−5849.

(21) Howard, W. L.; Brown, J. H., Jr. *J. Org. Chem.* **1961**, *26*, 1026−1028.

(22) Capon, B.; Smith, M. C. *J. Chem. Soc. B* **1969**, 1031−1033.

(23) Moreau, C.; Lecomte, J.; Mseddi, S.; Zmimita, N. *J. Mol. Catal. A: Chem.* **1997**, *125*, 143−149.

(24) Llàcer, E.; Romea, P.; Urpí, F. *Tetrahedron Lett.* **2006**, *47*, 5815−5818.

(25) Li, Y.-Q.; Wang, P.; Liu, H.; Lu, Y.; Zhao, X.-L.; Liu, Y. *Green Chem.* **2016**, *18*, 1798−1806.

(26) Wang, P.; Liu, H.; Li, Y.-Q.; Zhao, X.-L.; Lu, Y.; Liu, Y. *Catal. Sci. Technol.* **2016**, *6*, 3854−3861.

(27) Kannan, S.; Kumar, K. N.; Ramesh, R. *Polyhedron* **2008**, *27*, 701−708.

(28) Jeulin, S.; Duprat de Paule, S.; Ratovelomanana-Vidal, V.; Genêt, J.-P.; Champion, N.; Dellis, P. *Angew. Chem., Int. Ed.* **2004**, *43*, 320−325.

(29) Zhou, C.; Zhang, J.; Đaković, M.; Popović, Z.; Zhao, X.; Liu, Y. *Eur. J. Inorg. Chem.* **2012**, *2012*, 3435−3440.

(30) Sheldrick, G. M. *SHELXS-97*; Georg-August-Universität Göttingen: Göttingen, Germany, 1990.